Wash-Free Multi-Target Super-Resolution Microscopy with Photocaged DNA Labels

Nina Kaltenschnee[a,#], Marina S. Dietz[b,#], Laurell F. Kessler[b], Yunqing Li[b], Janik Kaufmann[a], Alexander Heckel[a,*], Mike Heilemann[b,*]

[a]Institute of Organic Chemistry and Chemical Biology, Goethe University Frankfurt, Frankfurt am Main, Germany
[b]Institute of Physical and Theoretical Chemistry, Goethe University Frankfurt, Frankfurt am Main, Germany

[#]These authors contributed equally.

[*]Correspondence: heckel@uni-frankfurt.de, heilemann@chemie.uni-frankfurt.de

Abstract

Super-resolution microscopy with DNA-fluorophore labels is primed for multi-target imaging of cell biological samples. However, direct interaction with the sample is required to exchange or add DNA-fluorophore labels in each imaging round, which can impair the accuracy of the imaging data at the nanometer scale. To bypass this requirement, we introduce a wash-free method that employs DNA oligonucleotides equipped with photocaging groups. Irradiation with light removes these photo-modulatable groups and changes the hybridization properties of DNA labels, enabling light-modulated targeting. We demonstrate this concept by imaging various cellular targets with confocal microscopy, single-molecule localization microscopy, and stimulated emission depletion (STED) microscopy.

Introduction

Super-resolution microscopy has revolutionized our understanding of cell biology.(Danial 2025) To capture the full context of subcellular architecture, imaging multiple targets within a sample is essential. Given that only a limited number of fluorophores can be distinguished based on their optical properties, this limitation has driven the development of sequential imaging strategies to increase the number of accessible targets in an experiment. This can, for example, be realized with chemical strategies that remove and replace fluorophore labels, as demonstrated in single-molecule localization microscopy.(Schroeter et al. 2025; Klevanski et al. 2020) Alternatively, fluorophore labels with transient, weak binding affinities to their target allow multi-target imaging through iterative exchange steps coupled with washing.(Albertazzi and Heilemann 2023) Examples are short, transiently hybridizing and fluorophore-labeled DNA oligonucleotides, as in DNA-point accumulation for nanoscale topography (DNA-PAINT),(Jungmann et al. 2014) weak-affinity fluorophore labels for self-labeling enzymes,(Kompa et al. 2023, 2025) and small-molecule fluorophore labels.(Spahn et al. 2018) Notably, these labeling strategies are compatible with various modalities of super-resolution microscopy.(Kompa et al. 2023; Glogger et al. 2022; Spahn et al. 2019; Glogger et al. 2021)

Fluorophore-labeled DNA in combination with sequence design has demonstrated many-target fluorescence imaging of complex molecular samples.(Unterauer et al. 2024; Schueder et al. 2024) One remaining challenge of these strategies is that either washing steps are needed, or molecular components need to be added to and mixed with the imaging buffer. Such direct interaction with the sample introduces an additional step in the experimental workflow and may perturb the nanoscale architecture of cellular samples. This, in turn, affects the information content that would otherwise be accessible with the excellent spatial resolution that these methods can achieve. To mitigate this limitation, we sought a new approach to multi-target imaging using DNA-fluorophore labels that is truly wash-free and does not require any physical interaction with the sample. We achieved this by integrating photo-modulatable groups (photocages) into short DNA sequences, which enabled the modulation of the hybridization properties through the illumination with light. Light acts as a non-invasive tool offering the necessary spatio-temporal control over a biological system of interest.(Brieke et al. 2012; Mangubat-Medina and Ball 2021) Such photocages have previously been used in the DNA hairpin structures to modulate the cellular activity of short DNA oligonucleotides.(Sambandan et al. 2017; Lucas et al. 2017) Here, we report the integration of photocages in short DNA oligonucleotides and demonstrate wash-free switching between imaging targets using light. We demonstrate this concept for confocal microscopy, single-molecule localization microscopy (SMLM), and stimulated emission depletion (STED) microscopy.

Results and Discussion

The coumarin photocage derivative methyl-7-(diethylamino)coumarin-4-ylmethyl (Me-DEACM) was chosen for the construction of photo-modulatable DNA oligonucleotides. Coumarin photocages release their payload by irradiation with visible light and in a well-behaved manner, minimizing cell damage.(Weinstain et al. 2020) For application in oligonucleotides, commercially available phosphoramidites are available. Thus, coumarin photocages are commonly applied and have previously been used masking the function of oligonucleotides e.g., to modulate mRNA translation,(Bollu et al. 2023) monitor mRNA transport in neurons,(Klimek et al. 2021) or to gain insights into zebrafish embryo development by light-regulation of proteins.(Brown et al. 2023) The absorption maximum in the blue-violet spectral region is orthogonal to commonly employed orange- and red-absorbing fluorophores in fluorescence microscopy.

In this work, we selected a methylated DEACM photocage, as it provides a slightly higher uncaging quantum yield compared to the unmodified DEACM.(Schulte et al. 2022) We opted for two orthogonal, photocaged oligonucleotide docking strands that simultaneously alter their hybridization properties upon irradiation (**Figure 1A**). Docking strand **cP1$_a$** is in an active state (“ON”) before uncaging and allows hybridization with the imager strand P1 and imaging of the first target. At the same time, the imager strand cannot bind to docking strand **cP1$_b$** as the interaction is sterically hindered by the coumarin groups (“OFF”). After irradiation with violet light, the system is reversed: the photocages are released, and **cP1$_a$** internally hybridizes, yielding a closed, inactive docking strand (“OFF”), while **cP1$_b$** adopts an active conformation, enabling imaging of the second target (“ON”).

Synthesis

The chemical synthesis (**Scheme 1**) started with a Grignard reaction of **1,** affording the methylated DEACM **2**. Next, **2** was reacted with the activated dT derivative **S3** (**Scheme S1**) to attach the coumarin moiety to the O4 and hence inhibit H-bonds between the nucleobases. Here, it is important to verify that the coumarin is connected to O4 using NMR, as in the case of attachment to N3, the rate of photolysis is strongly decreased. With the right isomer in hand, the tert-butyldimethylsilyl (TBDMS) protecting groups of **3** were cleaved, followed by attachment of dimethoxytrityl (DMTr) protecting group to the 5' position and finally phosphitylation to obtain the caged thymidine **4**. A comprehensive description of the synthesis is found in the **Supporting Information**. Compound **4** was then used in the solid-phase synthesis of the oligonucleotides. Both oligonucleotides were designed to contain the widely used P1-docking strand sequence.(Jungmann et al. 2014; Schnitzbauer et al. 2017; Narayanasamy et al. 2022; Oleksiievets et al. 2022) For **cP1$_b$**, three positions were chosen to introduce caged dT **4** and consequently disable hybridization with an imager strand (**Figure 1A**). For **cP1$_a$**, the P1 docking strand was extended with a fully complementary sequence containing three caged dTs to ensure complete internal hybridization after irradiation. Post-synthetically, an azide modification (**Figure S5**) was introduced for antibody labelling.

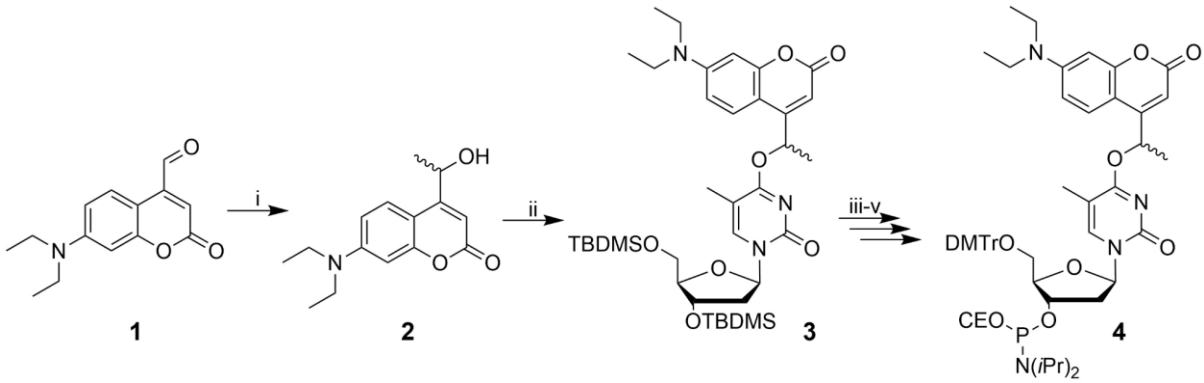

Scheme 1: Synthesis of Methyl-DEACM caged dT-Phosphoramidite **4**. i. MeMgBr, THF, -78 °C to rt, 21 h, 41%. ii. **S3**, DBU, ACN, rt, 20 h, 77%. iii. TBAF, AcOH, THF, 0 °C to rt, 20 h, 85%. iv. DMTr-Cl, DIPEA, DCM, 0 °C to rt, on, 83%. v. PN(iPr)$_2$(CEO)-Cl, DIPEA, DCM, 0 °C to rt, 1.5 h, 80%.

Caged Docking Strands for Wash-Free Multiplexed Fluorescence Microscopy

The caged docking strands **cP1$_a$** and **cP1$_b$** (**Figure 1A**) were conjugated to secondary antibodies via click chemistry (see **Experimental Procedures**) and used to label two distinct cellular structures by immunofluorescence. The first target was immunolabeled with **cP1$_a$** and imaged by transiently hybridizing to a fluorophore-labeled P1 imager strand. To switch from the first to the second target, low-intensity illumination with violet light (405 nm) was applied, which removes the Methyl-DEACM caging groups from **cP1$_a$** and **cP1$_b$**. This leads to an intramolecular hybridization of **cP1$_a$**, rendering it inaccessible for imaging, and makes **cP1$_b$** accessible for imaging the second target with the same fluorophore-labeled P1 imager strand (**Figure 1B**). In contrast to Exchange-DNA-PAINT,(Jungmann et al. 2014) no exchange of the imager strand is necessary for imaging the second target.

To validate the functionality of the caged docking strands, docking-strand–conjugated antibodies were used to label individual targets in U-2 OS cells (**Figure 1C**). α-tubulin was labeled with the deactivatable docking strand **cP1$_a$**, and confocal imaging showed the

expected microtubule network before uncaging. Upon illumination with very low intensity (< 100 W/cm^2, single frame) of 405 nm light, the tubulin signal disappeared, demonstrating highly efficient uncaging. TOM20 was labeled using the photoactivatable docking strand **cP1$_b$**, and the mitochondrial network became visible only after uncaging. Again, a single frame with 405 nm illumination was sufficient to reveal the mitochondrial structure.

After confirming that both docking strands were efficiently switched between their "ON" and "OFF" states, we labeled microtubules and mitochondria within the same sample and demonstrated that both structures can be visualized (**Figure 1D**). During uncaging, the transition from the microtubule to mitochondrial signal was clearly observable (**Figure S1A** and **Video S1**). The **cP1$_a$/cP1$_b$** system was subsequently applied to additional cellular targets (**Figure S1B–D**).

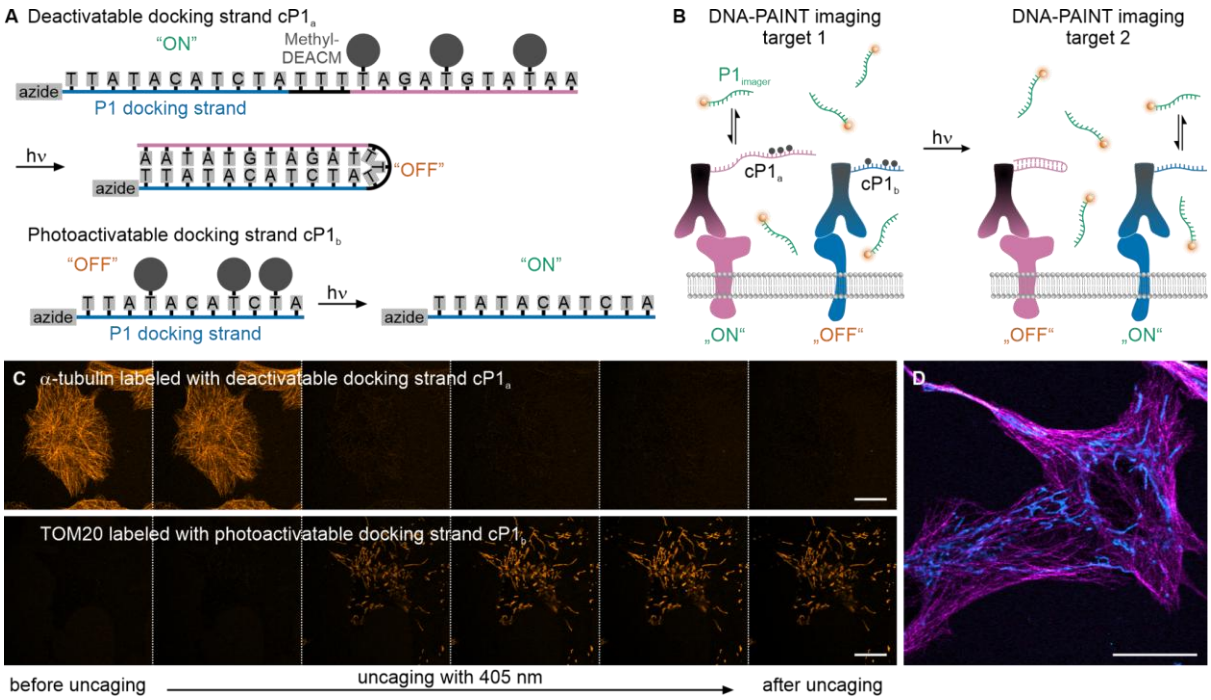

Figure 1. No-wash DNA-PAINT using caged docking strands. (A) Design of the photodeactivatable and photoactivatable docking strands **cP1$_a$** and **cP1$_b$**. Initially, **cP1$_a$** is accessible for hybridization to the complementary P1 imager strand, while **cP1$_b$** remains in its "OFF" state. Upon 405 nm illumination, the Methyl-DEACM cage groups are removed: **cP1$_a$** adopts a closed, inactive ("OFF") conformation, whereas **cP1$_b$** becomes activated and available for P1 imager binding. (B) Scheme of the no-wash two-target imaging workflow. Each target is labeled with either **cP1$_a$** or **cP1$_b$**, and images are recorded before and after 405 nm illumination. (C) Confocal images of α-tubulin labeled with **cP1$_a$** (top) show loss of microtubule signal during illumination with violet light. Confocal images of TOM20 labeled with **cP1$_b$** (bottom) show the appearance of the mitochondrial signal following illumination. All images were acquired using 100 nM P1-Cy3B imager strand. (D) Two-target confocal imaging of microtubules (magenta) and mitochondria (cyan). α-Tubulin was labeled with **cP1$_a$**, and TOM20 with **cP1$_b$**. The two-target image was generated by combining images recorded before and after violet-light illumination. Imager strand concentration was 100 nM P1-Cy3B. Scale bars 20 µm.

Next, we tested the compatibility of the caged docking strands with additional cellular stains across the visible spectrum. Microtubules and vimentin were labeled using **cP1$_a$** and **cP1$_b$**, respectively. Additionally, actin was stained with ATTO 488-phalloidin and mitochondria with MitoTracker Orange. This configuration enabled the imaging of four distinct targets using only three spectral channels (**Figure 2A**), demonstrating that caged docking strands can expand the number of addressable targets in otherwise spectrally limited experiments.

To show the applicability of caged docking strands to super-resolution microscopy, two-target DNA-PAINT experiments were performed (**Figure 2B**, **Figure S2**). Microtubules and ER were labeled with **cP1$_a$** and **cP1$_b$**, respectively. First, α-tubulin was imaged using a P1-Cy3B imager strand. After recording the first DNA-PAINT movie, the photocages were removed by illuminating the cell for 2 min with 405 nm light. Next, the KDEL sequence residing in the ER was imaged using the same imager strand. The two-target super-resolution image shows the nanoscale co-organization of microtubules and ER (**Figure 2Bi,ii**), in line with previous reports that the ER interacts with microtubules, sliding along stable, acetylated microtubules to help regulate ER positioning and organelle distribution.(Friedman et al. 2010; Zheng et al. 2021)

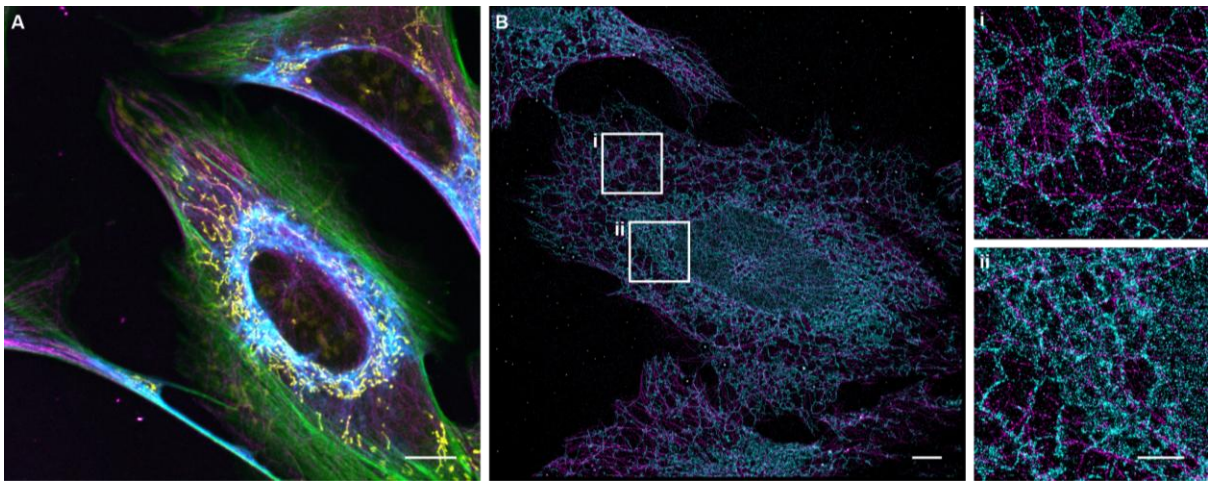

Figure 2. (A) Multiplexed confocal imaging of microtubules, vimentin, actin, and mitochondria in U-2 OS cells. α-tubulin (magenta) and vimentin (cyan) were labeled via immunofluorescence using **cP1$_a$** and **cP1$_b$** conjugated secondary antibodies, respectively, in combination with 50 nM P1(11nt)-ATTO 655. Actin was stained with ATTO 488-Phalloidin (green) and mitochondria with MitoTracker Orange (yellow). Scale bar 10 µm. (B) Two-target DNA-PAINT imaging of microtubules and ER in U-2 OS cells with caged docking strands. α-tubulin was labeled with **cP1$_a$** (magenta), and KDEL was labeled with **cP1$_b$** (cyan). 2 nM P1(9nt)-Cy3B imager strand was used for imaging. Before imaging the second target, the cell was illuminated for 2 min with 405 nm light. The NeNA localization precision for the DNA-PAINT image of α-tubulin was 5.33 nm, and for KDEL 5.47 nm. Scale bar 5 µm, zoom-ins 2 µm.

DNA-fluorophore labels were previously used for STED microscopy.(Spahn et al. 2019; Beater et al. 2015) We found that caged docking strands are equally applicable, and demonstrated two-target STED imaging using **cP1$_a$** and **cP1$_b$** (**Figure S3, Supporting Note 1**). To increase the signal-to-background ratio, we used self-quenched imager strands dual-labeled with Cy3B, which have a lower background fluorescence signal in the unbound state and show an increase in fluorescence signal upon binding to the complementary docking strand.(Kessler et al. 2024, 2023) Hence, two-target STED microscopy using a single type of imager strand was possible (**Figure S3**), which adds a new promising strategy for multi-target super-resolution microscopy.

Conclusion

We introduce cagePAINT as a strategy for wash-free, multi-target high-resolution imaging. By integrating photocages into DNA oligonucleotides, we demonstrate two-target confocal, DNA-PAINT, and STED microscopy using a single fluorophore-labeled imager strand. The highly efficient uncaging process triggered by violet light allows locally confined conversion, enabling dual-target imaging on a cell-by-cell basis and accelerating DNA-PAINT acquisition by

eliminating the need for washing steps between imaging rounds. The current design of caged oligonucleotides can be extended in various ways, for example, by including spectrally orthogonal caging groups or by implementing more complex and modular designs of oligonucleotides.(Schueder et al. 2024; Unterauer et al. 2024) The concept of photocages for multi-target imaging is not limited to DNA-fluorophore labels, and can be extended to photocaged self-labelling enzymes.(Walterspiel et al. 2025) The integration into other microscopy modalities, such as structured-illumination microscopy (SIM) or MINFLUX, is possible.(Radmacher et al. 2025) In summary, cagePAINT is economical, as only a single type of imager strand is used. Light triggering eliminates physical distortions and sample drift that can occur during washing in multiplexed DNA-PAINT experiments, and that increases the accuracy of super-resolution structural data.

Supporting Information

The authors have cited additional references within the Supporting Information.(Seyfried et al. 2017; Edelstein et al. 2014)

Acknowledgements

We thank Petra Freund for assistance with cell culture, Tanja Menche for helpful discussions, and Jonathan Marheineke for assistance in chemical synthesis. We gratefully acknowledge funding by the Deutsche Forschungsgemeinschaft (DFG, German Research Foundation) through CRC 1507, DFG INST 161/926-1 FUGG, DFG INST 161/778-1 FUGG, and DFG INST 161/1162-1 FUGG.

Keywords

DNA-PAINT, light control, multiplexed imaging, photocages, single-molecule localization microscopy,

References

Albertazzi, Lorenzo, and Mike Heilemann. 2023. “When Weak Is Strong: A Plea for Low-Affinity Binders for Optical Microscopy.” *Angewandte Chemie (International Ed. in English)* 62 (35): e202303390.

Beater, Susanne, Phil Holzmeister, Birka Lalkens, and Philip Tinnefeld. 2015. “Simple and Aberration-Free 4color-STED--Multiplexing by Transient Binding.” *Optics Express* 23 (7): 8630–8638.

Bollu, Amarnath, Nils Klöcker, Petr Špaček, Florian P Weissenboeck, Sabine Hüwel, and Andrea Rentmeister. 2023. “Light-Activated Translation of Different mRNAs in Cells via Wavelength-Dependent Photouncaging.” *Angewandte Chemie (International Ed. in English)* 62 (5): e202209975.

Brieke, Clara, Falk Rohrbach, Alexander Gottschalk, Günter Mayer, and Alexander Heckel. 2012. “Light-Controlled Tools.” *Angewandte Chemie (International Ed. in English)* 51 (34): 8446–8476.

Brown, Wes, Joshua Wesalo, Subhas Samanta, et al. 2023. “Genetically Encoded Aminocoumarin Lysine for Optical Control of Protein-Nucleotide Interactions in Zebrafish

Embryos.” *ACS Chemical Biology* 18 (6): 1305–1314.

Danial, John S. H. 2025. “Super-Resolution Microscopy for Structural Biology.” *Nature Methods* 22 (8): 1636–1652.

Edelstein, Arthur D., Mark A. Tsuchida, Nenad Amodaj, Henry Pinkard, Ronald D. Vale, and Nico Stuurman. 2014. “Advanced Methods of Microscope Control Using μManager Software.” *Journal of Biological Methods* 1 (2). https://doi.org/10.14440/jbm.2014.36.

Friedman, Jonathan R., Brant M. Webster, David N. Mastronarde, Kristen J. Verhey, and Gia K. Voeltz. 2010. “ER Sliding Dynamics and ER–mitochondrial Contacts Occur on Acetylated Microtubules.” *Journal of Cell Biology* 190 (3): 363–375.

Glogger, Marius, Christoph Spahn, Jörg Enderlein, and Mike Heilemann. 2021. “Multi-Color, Bleaching-Resistant Super-Resolution Optical Fluctuation Imaging with Oligonucleotide-Based Exchangeable Fluorophores.” *Angewandte Chemie (International Ed. in English)* 60 (12): 6310–6313.

Glogger, Marius, Dongni Wang, Julian Kompa, et al. 2022. “Synergizing Exchangeable Fluorophore Labels for Multitarget STED Microscopy.” *ACS Nano* 16 (11): 17991–17997.

Jungmann, Ralf, Maier S. Avendaño, Johannes B. Woehrstein, Mingjie Dai, William M. Shih, and Peng Yin. 2014. “Multiplexed 3D Cellular Super-Resolution Imaging with DNA-PAINT and Exchange-PAINT.” *Nature Methods* 11 (3): 313–318.

Kessler, Laurell F., Ashwin Balakrishnan, Nina S. Deußner-Helfmann, et al. 2023. “Self-Quenched Fluorophore Dimers for DNA-PAINT and STED Microscopy.” *Angewandte Chemie (International Ed. in English)* 62 (39): e202307538.

Kessler, Laurell F., Ashwin Balakrishnan, Tanja Menche, et al. 2024. “Self-Quenched Fluorophore-DNA Labels for Super-Resolution Fluorescence Microscopy.” *The Journal of Physical Chemistry. B* 128 (28): 6751–6759.

Klevanski, Maja, Frank Herrmannsdoerfer, Steffen Sass, Varun Venkataramani, Mike Heilemann, and Thomas Kuner. 2020. “Automated Highly Multiplexed Super-Resolution Imaging of Protein Nano-Architecture in Cells and Tissues.” *Nature Communications* 11 (1): 1552.

Klimek, Robin, Paul G. Donlin-Asp, Claudio Polisseni, Vanessa Hanff, Erin M. Schuman, and Alexander Heckel. 2021. “Visible Light-Activatable Q-Dye Molecular Beacons for Long-Term mRNA Monitoring in Neurons.” *Chemical Communications (Cambridge, England)* 57 (94): 12683–12686.

Kompa, Julian, Jorick Bruins, Marius Glogger, et al. 2023. “Exchangeable HaloTag Ligands for Super-Resolution Fluorescence Microscopy.” *Journal of the American Chemical Society* 145 (5): 3075–3083.

Kompa, Julian, Lars Jeremy Dornfeld, Nicola Porzberg, et al. 2025. “Fast, Bright and Reversible Rhodamine Tags for Live-Cell Imaging.” In *bioRxiv*. July 9. https://doi.org/10.1101/2025.07.06.663254.

Lucas, Tina, Florian Schäfer, Patricia Müller, Sabine A. Eming, Alexander Heckel, and Stefanie Dimmeler. 2017. “Light-Inducible antimiR-92a as a Therapeutic Strategy to Promote Skin Repair in Healing-Impaired Diabetic Mice.” *Nature Communications* 8 (May): 15162.

Mangubat-Medina, Alicia E., and Zachary T. Ball. 2021. “Triggering Biological Processes: Methods and Applications of Photocaged Peptides and Proteins.” *Chemical Society Reviews* 50 (18): 10403–10421.

Narayanasamy, Kaarjel K., Johanna V. Rahm, Siddharth Tourani, and Mike Heilemann. 2022. “Fast DNA-PAINT Imaging Using a Deep Neural Network.” *Nature Communications* 13 (1): 5047.

Oleksiievets, Nazar, Yelena Sargsyan, Jan Christoph Thiele, et al. 2022. “Fluorescence Lifetime DNA-PAINT for Multiplexed Super-Resolution Imaging of Cells.” *Communications Biology* 5 (1): 38.

Radmacher, Niels, Alexey I. Chizhik, Oleksii Nevskyi, José Ignacio Gallea, Ingo Gregor, and Jörg Enderlein. 2025. “Molecular Level Super-Resolution Fluorescence Imaging.” *Annual Review of Biophysics* 54 (1): 163–184.

Sambandan, Sivakumar, Güney Akbalik, Lisa Kochen, et al. 2017. “Activity-Dependent Spatially Localized miRNA Maturation in Neuronal Dendrites.” *Science (New York, N.Y.)* 355 (6325): 634–637.

Schnitzbauer, Joerg, Maximilian T. Strauss, Thomas Schlichthaerle, Florian Schueder, and Ralf Jungmann. 2017. “Super-Resolution Microscopy with DNA-PAINT.” *Nature Protocols* 12 (6): 1198–1228.

Schroeter, Helene Gregoria, Steffen Sass, Mike Heilemann, Thomas Kuner, and Maja Klevanski. 2025. “Nanoscale Mapping of the Subcellular Glycosylation Landscape.” *Advanced Science (Weinheim, Baden-Wurttemberg, Germany)*, November 10, e06731.

Schueder, Florian, Felix Rivera-Molina, Maohan Su, et al. 2024. “Unraveling Cellular Complexity with Transient Adapters in Highly Multiplexed Super-Resolution Imaging.” *Cell* 187 (7): 1769–1784.e18.

Schulte, Albert M., Georgios Alachouzos, Wiktor Szymański, and Ben L. Feringa. 2022. “Strategy for Engineering High Photolysis Efficiency of Photocleavable Protecting Groups through Cation Stabilization.” *Journal of the American Chemical Society* 144 (27): 12421–12430.

Seyfried, Patrick, Laura Eiden, Nikolai Grebenovsky, Günter Mayer, and Alexander Heckel. 2017. “Photo-Tethers for the (Multi-)Cyclic, Conformational Caging of Long Oligonucleotides.” *Angewandte Chemie (International Ed. in English)* 56 (1): 359–363.

Spahn, Christoph, Florian Hurter, Mathilda Glaesmann, Christos Karathanasis, Marko Lampe, and Mike Heilemann. 2019. “Protein-Specific, Multicolor and 3D STED Imaging in Cells with DNA-Labeled Antibodies.” *Angewandte Chemie (International Ed. in English)* 58 (52): 18835–18838.

Spahn, Christoph K., Mathilda Glaesmann, Jonathan B. Grimm, Anthony X. Ayala, Luke D. Lavis, and Mike Heilemann. 2018. “A Toolbox for Multiplexed Super-Resolution Imaging of the E. Coli Nucleoid and Membrane Using Novel PAINT Labels.” *Scientific Reports* 8 (1): 14768.

Unterauer, Eduard M., Sayedali Shetab Boushehri, Kristina Jevdokimenko, et al. 2024. “Spatial Proteomics in Neurons at Single-Protein Resolution.” *Cell* 187 (7): 1785–1800.e16.

Walterspiel, Franziska, Begoña Ugarte-Uribe, Jonas Weidenhausen, et al. 2025. “A

Photoswitchable HaloTag for Spatiotemporal Control of Fluorescence in Living Cells." *Angewandte Chemie (International Ed. in English)*, October 23, e202424955.

Weinstain, Roy, Tomáš Slanina, Dnyaneshwar Kand, and Petr Klán. 2020. "Visible-to-NIR-Light Activated Release: From Small Molecules to Nanomaterials." *Chemical Reviews* 120 (24): 13135–13272.

Zheng, Pengli, Christopher J. Obara, Ewa Szczesna, et al. 2021. "ER Proteins Decipher the Tubulin Code to Regulate Organelle Distribution." *Nature* 601 (7891): 132–138.